Reflection and Transmission coefficient for VTI media

R. K. Sharma and R. J. Ferguson

ABSTRACT

Presently, we obtain the reflection (R) and transmission (T) coefficients of plane waves at boundary between two transverse anisotropic media with the vertical axis of symmetry (VTI) in behalf of its importance for numerical computations. Additionally, these coefficients are valuable for the full elastic wave modelling in anisotropic media. Classical R and T coefficients have been obtained in terms of phase angle and can be computed by using the effective ray parameter. To do this, we compute a normal for each individual plane wave based on local velocity, that is function of Thomson's parameter of the medium, and a vector cross-product of this normal with the normal to the reflector yields a ray parameter that is used here to compute the corresponding R and T coefficients for a given plane wave. Further, the importance of the Thomson's parameters in order to understand the seismic waves signatures in anisotropic media make it necessary to obtain R and T coefficients in Thomson's parameters. For doing so, we build a relationship between Vigot elastic constants and Thomson's parameters by following Graebner's approach. Using this relationship, the corresponding R and T coefficients are obtained in terms of Thomson's parameters. Another importance of this approach is the automatic adaption of R and T coefficients for the transverse anisotropic media with the horizontal axis of symmetry (HTI). Moreover, amplitude versus offset (AVO) is a variation in seismic reflection amplitude with offset and it's also referred as AVA (amplitude versus angle). Typically, amplitude decreases with offset because of geometric spreading, attenuation and other factors while an AVO anomaly is characterized by the increasing AVO in a sedimentary section and indicates the probability of the presence of hydrocarbons. As opposed to the isotropic case where the velocity remains constant for all incident angles, the velocity is the function of the angle of incidence for anisotropic media and motivates author to analyze the effect of rock anisotropy on the R and T coefficients of seismic waves. To achieve this purpose, first SH wave is considered, due to its simplicity for VTI media. The effect of Thomson parameter γ on the R coefficients is delineated presently. In continuing of this, the three models characterized by the Class 1, 2 and 3 type of Gas-sand anomaly are considered for observing the influence of anisotropy on P-wave reflectivity and to test the accuracy of the plane wave R coefficients. A test of accuracy of the popular Rüger's approximation is also delineated here.

INTRODUCTION

The travel time of a signal from the surface to and from a reflector and the amplitude of the reflection comprise the seismic response. Since the reflection coefficient play an important role in order to interpret the field records for lithology, porosity and fluid content etc (Upadhyay, 2004). Thus, the amplitude of the reflection attains more attention of Geoscientists. For isotropic media, the amplitude of the reflection is a function of the density, compressional and shear wave velocities of the two layers that make up the interface and the angle of incidence (Shearer, 1999). The velocity of isotropic media remains constant during the AVO analysis while velocity of anisotropic media varies with angle of incidence and interrupt the AVO analysis (Rüger, 2001). In order to analyze the effect of anisotropy

on the R and T coefficients, VTI model is taken into account due to its simplicity among anisotropic media beyond the isotropic media. The thinly layered media with horizontal interfaces and horizontally stratified shale formations are characterized by the VTI model (Thomson, 2002). For VTI media the wave equation separates into a coupled pair of the equations for the P-SV waves and into a single equation for the pure SH-wave (Slawinski, 2003). Further, VTI media possess z axis as axis of symmetry so there is no loss of generality in considering propagation in any plane. First we discuss about the plane wave R and T coefficients of SH wave for VTI media. Then we consider the plane wave R and T coefficients of P- and SV-wave as an extension of preceding work.

R AND T COEFFICIENTS OF SH-WAVE FOR VTI MEDIA

In past, R and T coefficients have been obtained in several domains according to their importance. Further, on consideration of anisotropy in seismic exploration, the R and T coefficients have been obtained in terms of the phase angle and material properties on the either side of the interface (Daley and Horn, 1977). Presently, we drive the R and T coefficients in the plane wave domain in behalf of the efficiency in terms of the computational time for Rayleigh Sommerfeld modelling(RSM) (Sharma and Ferguson, 2009). Along with this, some times R and T coefficients are required for use in reflectivity programs where integration over ray parameter is required (Rüger, 2001). For this case parametrization by the phase angle can be inconvenient. This inconvenience can be avoided by deriving the R and T coefficients in terms of the ray parameter. To do this, we compute the ray parameter using effective ray parameter approach (Sharma and Ferguson, 2009) and is used to compute corresponding R and T coefficients in the plane wave domain.

In general, the reflected and transmitted waves are generated by an incident wave when an interface is encountered. The amplitude of the reflected and transmitted waves depend on the R and T coefficients (Krebes, 2008). In order to obtain the R and T coefficients boundary conditions, the continuity of displacement and traction, are considered at the boundary. After applying the boundary conditions R and T coefficients for anisotropic media are obtained in terms of the effective ray parameter and the elastic constant and can be written as (Slawinski, 2003)

$$R_{SH} = \frac{c_{44}^1 \, q_1 - c_{44}^2 \, q_2}{c_{44}^1 \, q_1 + c_{44}^2 \, q_2}, \tag{1}$$

and

$$T_{SH} = \frac{2 \, c_{44}^1 \, q_1}{c_{44}^1 \, q_1 + c_{44}^2 \, q_2}, \tag{2}$$

where c_{44}^1 and c_{44}^2 are the elastic constants of the incident and the refracted media. c_{44}^1 can be related to Thomson's parameter as (Thomson, 2002)

$$c_{44}^1 = \rho_1 \, (\beta_{01})^2, \tag{3}$$

and c_{44}^2 is described as

$$c_{44}^2 = \rho_2 \, (\beta_{02})^2, \tag{4}$$

where ρ and β are the density and the vertical shear wave velocity. In subscript the first digit indicates the shear wave propagation direction with respect to the vertical and the second digit indicates the medium. The incident and the refracted medium are characterized

by indices 1 and 2, respectively. Following the equations 3 and 4, the reflection and transmission coefficients can be described as

$$R_{SH} = \frac{\rho_1 \, \beta_{01}{}^2 q_1 - \rho_2 \, \beta_{02}{}^2 q_2}{\rho_1 \, \beta_{01}{}^2 q_1 + \rho_2 \, \beta_{02}{}^2 \, q_2}, \tag{5}$$

and

$$T_{SH} = 2 \, \frac{\rho_1 \, \beta_{01}{}^2 q_1}{\rho_1 \, \beta_{01}{}^2 q_1 + \rho_2 \, \beta_2{}^2 q_2}, \tag{6}$$

where q_1 is the vertical slowness for SH wave in the incident medium and can be written as (Ferguson and Margrave, 2008)

$$q_1 = \sqrt{\beta_{01}{}^{-2} - p_I{}^2 \, (2 \, \gamma_1 + 1)}, \tag{7}$$

and the vertical slowness of the refracted medium q_2 is described as

$$q_2 = \sqrt{\beta_{02}{}^{-2} - p_I{}^2 \, (2 \, \gamma_2 + 1)}, \tag{8}$$

where γ_1 and γ_2 are the Thomson's parameters of the incident and the refracted media. p_I is the effective ray parameter and can be computed as

$$p_I = |\hat{\mathbf{p}} \times \hat{\mathbf{a}}| \, \sqrt{p_1^2 + p_2^2 + q^2}, \tag{9}$$

where p_1, p_2 and q are the horizontal components 1, 2 and the vertical component of the slowness vector, respectively and these are evaluated in the incident medium. The slowness vector $\hat{\mathbf{p}}$ characterizes the direction of the incident wavefield according to (Ferguson and Margrave, 2008),

$$\hat{\mathbf{p}} = \frac{p_1 \hat{\mathbf{i}} + p_2 \hat{\mathbf{j}} + q \hat{\mathbf{k}}}{\sqrt{p_1^2 + p_2^2 + q^2}}. \tag{10}$$

The unit normal vector $\hat{\mathbf{a}}$ associated with TTI symmetry plane is written as

$$\hat{\mathbf{a}} = \sin \theta_a \, \cos \phi_a \, \hat{\mathbf{i}} + \sin \theta_a \, \sin \phi_a \, \hat{\mathbf{j}} + \cos \theta_a \, \hat{\mathbf{k}}. \tag{11}$$

where θ_a and ϕ_a are the dip and azimuth of the normal to the interface respectively.

REFLECTION AND TRANSMISSION COEFFICIENTS FOR P-SV WAVE

Historically, the P-SV reflection and transmission coefficients of an isotropic media have been studied by numerous authors (Aki and Richards, 1980; Kennett, 2001). Further, Daley and Horn has extended this study for the anisotropic media (Daley and Horn, 1977). Using the zeroth order approximation to an asymptotic ray series they have published the displacement reflection and transmission coefficients of P-SV waves for VTI media in terms of the elastic coefficients and the phase angle (Daley and Horn, 1977). Accounting the importance of the plane wave reflection and transmission coefficients as delineated in the previous section, here we also derive plane wave P-SV reflection and transmission coefficients. Graebner (Graebner, 1992) has published the reflection and transmission coefficient in terms of the elastic coefficients and the horizontal and the vertical components

of the slowness vector . Since Thomson's parameters for an anisotropic medium play an important role in order to reduces the non uniqueness of the inverse problem where it is needed to model the data in a given geologic environment (Grechka, 2009). Thus, we derive the reflection and transmission coefficients in terms of Thomson's parameters for seeking the effect of Thomson's parameters (δ, ϵ) on these coefficients . To do this, we develop a relationship between the elastic constants used by Graebner (Graebner, 1992) and Thomson's parameters (Thomsen, 1986). Further, by using the effective ray parameter we obtain 3D reflection and transmission coefficients for VTI media.

To obtain the reflection and transmission coefficients, the continuity of the displacement and the stress is required. Consider a P-wave impinges on the interface and it generate the reflected and refracted P- and SV-waves at the interface. Then, the stress-strain relationship $(\tau = \mathbf{c}\epsilon)$ can be expressed as (Graebner, 1992)

$$
\begin{bmatrix} \tau_{xx} \\ \tau_{yy} \\ \tau_{zz} \\ \tau_{yz} \\ \tau_{zx} \\ \tau_{xy} \end{bmatrix} = \begin{bmatrix} A & A-2N & F & 0 & 0 & 0 \\ A-2N & A & F & 0 & 0 & 0 \\ F & F & C & 0 & 0 & 0 \\ 0 & 0 & 0 & L & 0 & 0 \\ 0 & 0 & 0 & 0 & L & 0 \\ 0 & 0 & 0 & 0 & 0 & N \end{bmatrix} \begin{bmatrix} \epsilon_{xx} \\ \epsilon_{yy} \\ \epsilon_{zz} \\ 2\,\epsilon_{yz} \\ 2\,\epsilon_{zx} \\ 2\,\epsilon_{xy} \end{bmatrix}, \tag{12}
$$

where $\epsilon_{ij} = \frac{1}{2}(\partial u_i/\partial x_j + \partial u_j/\partial x_i)$, and $i, j = x, y, z$ or 1,2,3. The τ_{ij} are the stresses, the ϵ_{ij} are the strains, the u_i are the components of particle displacement and the A, C, F, L and N are the elastic constants. Now, the substitution of the plane wave particle displacement equation into the wave equation yields the eigenvalues (phase velocities) of the P and SV-waves. Once the eigenvalues are known, the corresponding eigenvectors can be obtained as a function of the elastic coefficients and the horizontal and the vertical slownesses. On being acquainted with the eigenvalues and the eigenvectors of the P- and SV-waves, the reflection and the transmission coefficients are obtained after implementation of the boundary conditions at the interface and can be expressed in the matrix form as $\mathbf{Sx=b}$. For this case the matrix $\mathbf{S}$ is given by

$$
\mathbf{S} = \begin{bmatrix} l_{\alpha_1} & m_{\beta_1} & -l_{\alpha_2} & -m_{\beta_2} \\ m_{\alpha_1} & -l_{\beta_1} & m_{\alpha_2} & -l_{\beta_2} \\ a_1 & b_1 & a_2 & b_2 \\ c_1 & d_1 & -c_2 & -d_2 \end{bmatrix}, \tag{13}
$$

where $a_i = L_i(q_{\alpha_i} l_{\alpha_i} + p_I m_{\alpha_i})$, $b_i = L_i(q_{\beta_i} m_{\beta_i} - p_I l_{\beta_i})$, $c_i = p_I l_{\alpha_i} F_i + q_{\alpha_i} m_{\alpha_i} C_i$, and $d_i = p_I m_{\beta_i} F_i - q_{\beta_i} l_{\beta_i} C_i$, and $i=1$ corresponds to the upper medium and $i=2$ indicates the lower medium. The l_α, m_α are the eigenvectors of the P-wave and the l_β, m_β are the eigenvectors of the SV wave and can be expressed as

$$
l_k = \sqrt{\frac{(C'q_k^2 + L'p_I^2 - 1)}{(A'p_I^2 + L'q_k^2 - 1) + (C'q_k^2 + L'p_I^2 - 1)}}, \tag{14}
$$

and

$$
m_k = \sqrt{\frac{(A'p_I^2 + L'q_k^2 - 1)}{(A'p_I^2 + L'q_k^2 - 1) + (C'q_k^2 + L'p_I^2 - 1)}}, \tag{15}
$$

where $k=1$ characterize the P-wave and the SV is characterized by the $k=2$ and $A'=A/\rho$, $L'=L/\rho$, $C'=C/\rho$. Now the vectors, $\mathbf{x}$ and $\mathbf{b}$, are given by

$$\mathbf{x} = \begin{bmatrix} r_{pp} \\ r_{ps} \\ t_{pp} \\ tps \end{bmatrix}, \tag{16}$$

and

$$\mathbf{b} = \begin{bmatrix} -l_{\alpha_1} \\ m_{\alpha_1} \\ L_1 \left(q_1 \, l_{\alpha_1} + p_I m_{\alpha_1} \right) \\ -p_I l_{\alpha_1} \, F_1 - q_{\alpha_1} \, m_{\alpha_1} \, C_1 \end{bmatrix}. \tag{17}$$

In above equations the p_I is the effective ray parameter and computed with equation9. The q_α and the q_β are the vertical slowness of the P- and SV-waves, respectively and can be expressed as (Ferguson and Margrave, 2008)

$$q_\alpha = 1/2 \sqrt{2 \, \beta_0^{-2} + 2 \, \alpha_0^{-2} - 4 \, S p_I^2 - 4 \, R}, \tag{18}$$

and

$$q_\beta = 1/2 \sqrt{2 \, \beta_0^{-2} + 2 \, \alpha_0^{-2} - 4 \, S p_I^2 + 4 \, R}, \tag{19}$$

where

$$S = \left(1/2 \, \frac{\alpha_0^2}{\beta_0^2} + 1/2 \right) \epsilon + 1 - 1/2 \, \frac{\delta \, \alpha_0^2}{\beta_0^2}, \tag{20}$$

and

$$R = 1/2 \sqrt{4 \, p_I^4 \left(S^2 - 2 \, \epsilon - 1 \right) + 4 \, \frac{p_I^2 \, (2 \, \epsilon - S + 1)}{\beta_0^2} + 4 \, \frac{p_I^2 \, (1 - S)}{\alpha_0^2} + \beta_0^{-4} + \alpha_0^{-4} + 2 \, \frac{1}{\alpha_0^2 \beta_0^2}}. \tag{21}$$

However, the elastic coefficient matrix for VTI media can be expressed as (Tsvankin, 2001)

$$c_{VTI} = \begin{bmatrix} c_{11} & c_{11} - 2 \, c_{66} & c_{13} & 0 & 0 & 0 \\ c_{11} - 2 \, c_{66} & c_{11} & c_{13} & 0 & 0 & 0 \\ c_{13} & c_{13} & c_{33} & 0 & 0 & 0 \\ 0 & 0 & 0 & c_{44} & 0 & 0 \\ 0 & 0 & 0 & 0 & c_{44} & 0 \\ 0 & 0 & 0 & 0 & 0 & c_{66} \end{bmatrix}. \tag{22}$$

The comparison of elastic stiffness matrix from equation 12 with the above equation yields the relationship

$$c_{11} = A, c_{44} = L, c_{33} = C, c_{55} = L,$$

and

$$c_{12} = c_{11} - 2\,c_{66}. \tag{23}$$

Moreover, Thomson's parameters are defined as follow: The vertical P wave velocity is characterized by

$$\alpha_0 = \sqrt{\frac{c_{33}}{\rho}}, \tag{24}$$

and S wave velocity along the vertical axis of symmetry can be defined by

$$\beta_0 = \sqrt{\frac{c_{44}}{\rho}}, \tag{25}$$

and anisotropy can be characterized by the dimensionless coefficients

$$\epsilon = 1/2 \, \frac{c_{11} - c_{33}}{c_{33}}, \tag{26}$$

$$\gamma = 1/2 \, \frac{c_{66} - c_{44}}{c_{44}}, \tag{27}$$

and

$$\delta = 1/2 \, \frac{\left(c_{13} + c_{44}\right)^2 - \left(c_{33} - c_{44}\right)^2}{c_{33}\,\left(c_{33} - c_{44}\right)}. \tag{28}$$

By considering the equations (23 to 28), it can be demonstrated that

$$A = \rho\alpha_0^2(1 + 2\epsilon),\, C = \rho\alpha_0^2,\, L = \rho\beta_0^2,\, N = \rho\beta_0^2,$$

and

$$F = \rho\,\sqrt{\left(\alpha_0{}^2 - \beta_0{}^2\right)\left(\left(2\,\delta + 1\right)\alpha_0{}^2 - \beta_0{}^2\right)} - \rho\,\beta_0{}^2. \tag{29}$$

Once this relationship is build and is used in above equations, the corresponding R and T coefficients are obtained in Thomson's parameters.

EXAMPLE

Now following the equations from 1 to 11 as discussed above, we obtain the reflection and transmission coefficients of SH-wave in the plane wave domain for interfaces between two VTI media. To authenticate the proposed approach we obtain the reflection and transmission coefficients for a isotropic medium by employing a constraint on the γ $(\gamma = 0)$ in equations 5 and 6 since $\gamma=0$ corresponds to the isotropic medium. Figure 1 shows the real and imaginary part of the 3D reflection and transmission coefficients obtained as applying a constraint $\gamma=0$ on anisotropic algorithm. Figure 2 shows the 3D reflection and transmission coefficients by following the isotropic algorithm as discussed by author in the last year's CREWES report and it is the facsimile of the Figure 1. Further, the corroboration is attained by consider the in-line slices and the cross-line slices of the reflection and transmission coefficients and are shown in Figure 3a, b, c and d. The obtained results by following the anisotropic and isotropic algorithms are denoted by the red and the green colours, respectively, and the overlapping of these results ensure the efficacy of the proposed approach of obtaining R and T coefficients in the plane wave domain.
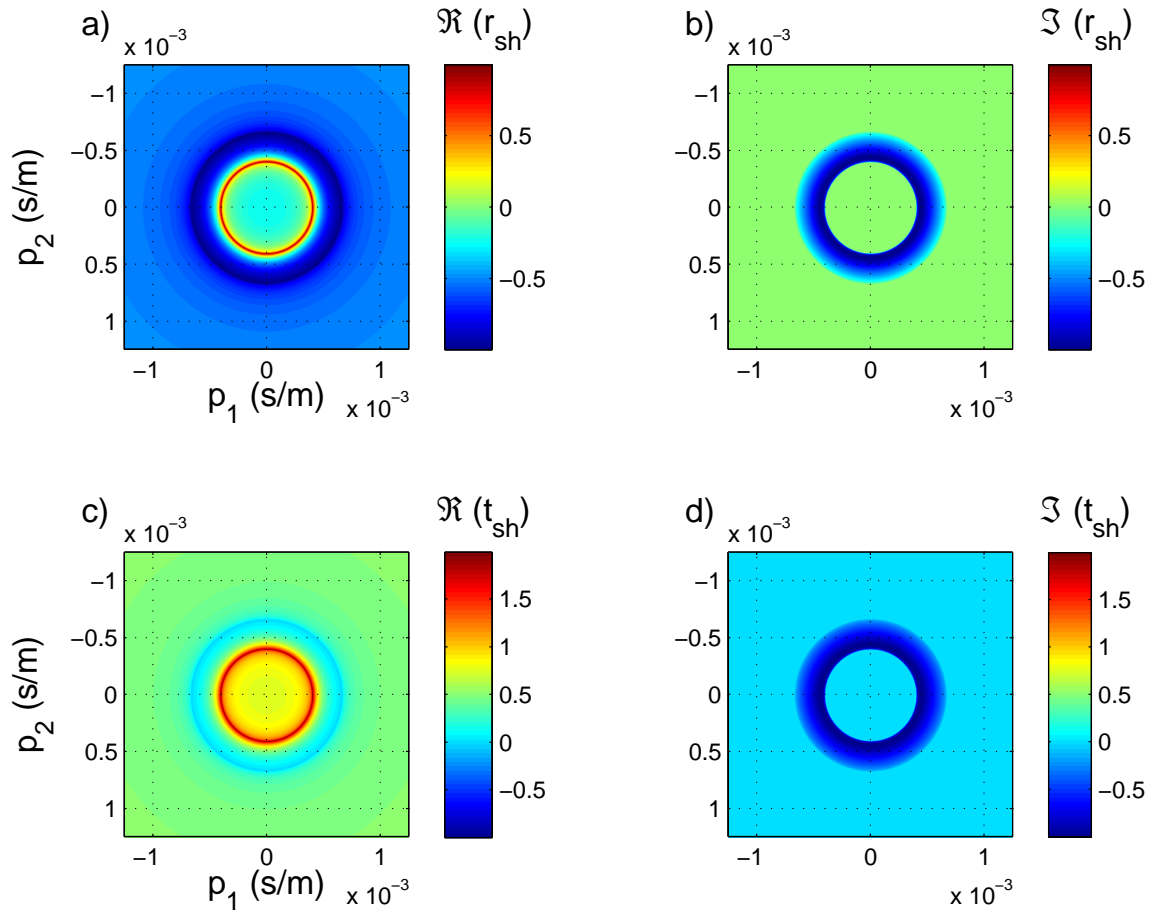
FIG. 1: a) Real part of reflection coefficient. b) Imaginary part of reflection coefficient. c) Real part of transmission coefficient. d) Imaginary part of transmission coefficient, obtained from the anisotropic algorithm by applying constraint $(\gamma = 0)$ on it.
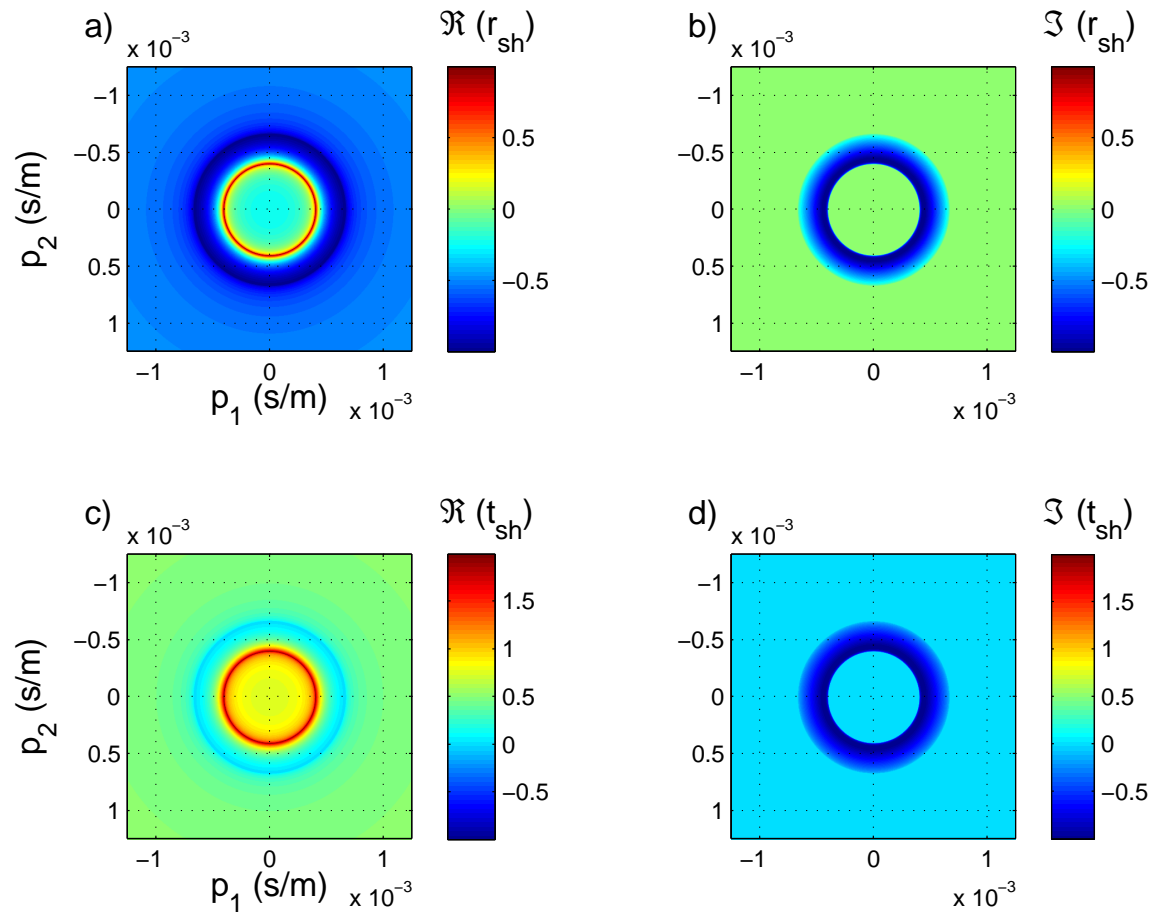
FIG. 2: a) Real part of reflection coefficient. b) Imaginary part of reflection coefficient. c) Real part of transmission coefficient. d) Imaginary part of transmission coefficient, obtained from the isotropic algorithm.
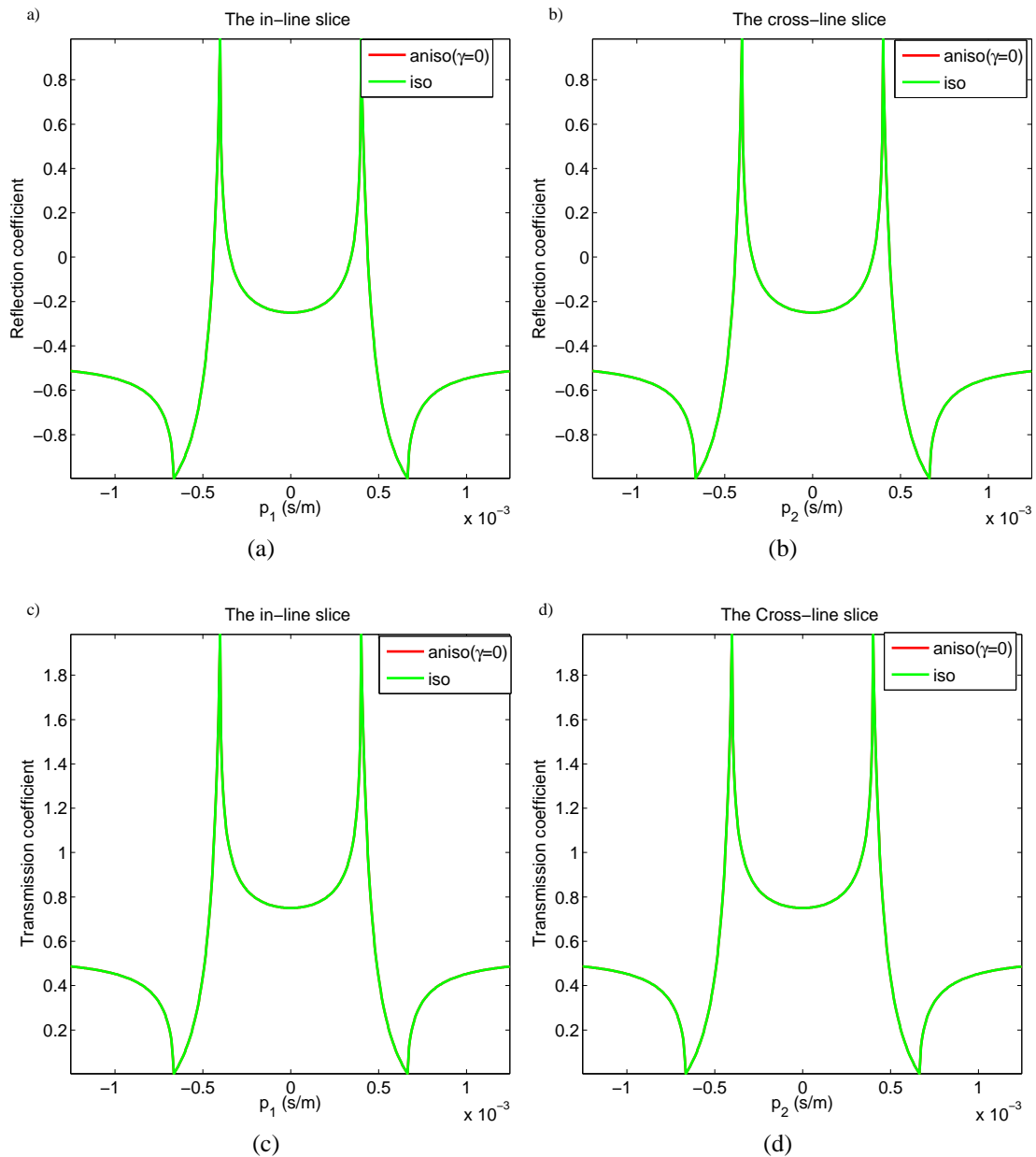
FIG. 3: (a) The in-line (b) The cross-line slices of the SH-wave *R* coefficients. (c) The in-line (d) The cross-line slices of the SH-wave *T* coefficients. The red line denotes the coefficients obtained by degenerated anisotropic algorithm and the green line shows the isotropic coefficients. The overlapping of these curve endorse the efficacy of the anisotropic algorithm for isotropic media.

As it is known that AVO analysis consider the amplitude variation for the precritical propagation (Rüger, 2001), we consider this condition in order to analyze the influence of Thomson's parameter on the AVO analysis. To do this, the upper medium is characterized by the invariant vertical velocity and the variable γ and the lower medium possesses the covariant Thomson's parameters. Now two cases for the lower medium : (1) when the vertical velocity of the lower medium exceeds the vertical velocity of the upper medium. (2) The reverse to the first case , are considered. Then, four sub-cases (i)$\gamma_1=\gamma_2=0$ (ii)$\gamma_1 \neq 0$ and $\gamma_2=0$ (iii)$\gamma_2 > \gamma_1$ (iv)$\gamma_2 < \gamma_1$ have been taken into account. Figure 4 shows the reflection coefficient curves as a function of the horizontal slowness for the first case with four sub-cases. It is seen that at zero slowness the reflected wave has negative amplitude as expected since the velocity of the lower medium is greater than the velocity of the upper medium. Then iso/iso curve follows the expected behaviour. While, the change between the reflection coefficient values, as well as the change of the slope of the reflection coefficient, is significant among the individual sub-cases for the first case. Only for zero slowness (normal incidence) do the curves coincide. The slope of the reflection coefficients for aniso/iso and anisoγ_1/aniso($\gamma_2 < \gamma_1$) sub-cases is less than the slope of the iso/iso. As $\gamma > 0$ corresponds to the velocity increment with slowness, for aniso/iso situation the velocity of the upper medium increases with slowness while lower medium's velocity remains constant hence the numerator of the equation 5 attains the less value and denominator get more value than the values obtained for iso/iso situation. The both factors, together, allow us to except the obtained pattern of the reflection coefficient curve. Further, for anisoγ_1/aniso($\gamma_2 < \gamma_1$) scenario, the obtained reflection coefficient curve lies in between the previous two situation. The obtained reflection coefficient curve for the fourth sub-case shows the more deviation from the obtained curve of the isotropic-isotropic situation as the velocity of the lower medium increases more rapidly than upper medium in this case.
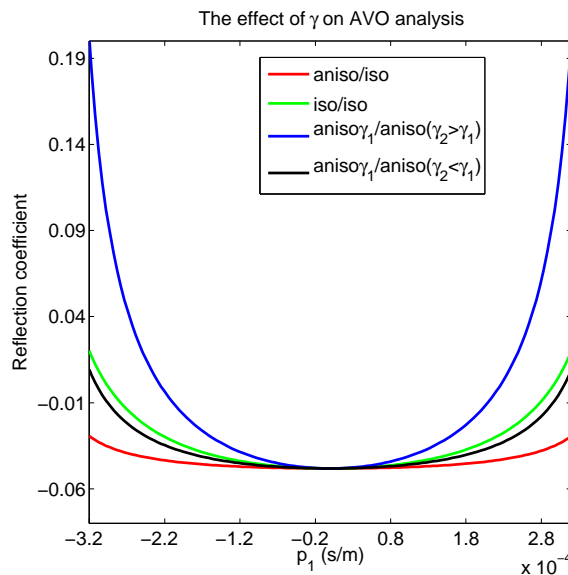
FIG. 4: The variation of R coefficient with horizontal slowness for the different interfaces illustrates that anisotropy does have a considerable influence on the AVO analysis.

Figure 5 shows the reflection coefficient curves as a function of the horizontal slowness for the second case with four sub-cases. Again the change between the reflection coeffi-
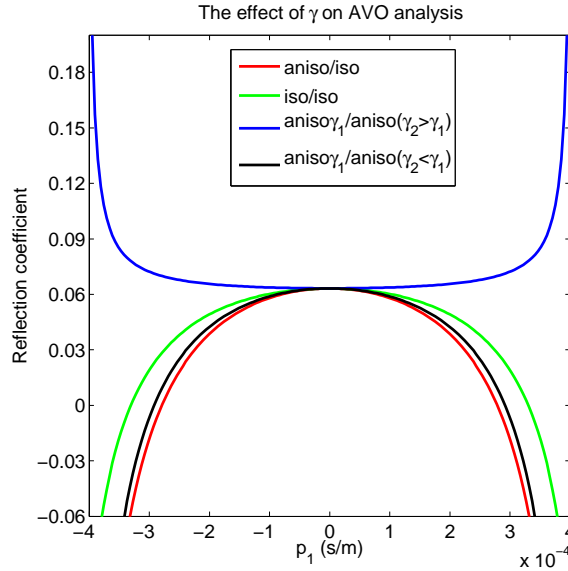
FIG. 5: The influence of the Thomson's parameter γ on the AVO analysis as shown in Figure 4 for different model.

cient values, as well as the change of the slope of the reflection coefficient, is significant among the individual sub-cases. However, as indicated in the above examples, ignoring the presence of anisotropy in VTI media has the potential of severely distorting the AVO analysis.

Now following the theory delineated above in the reflection and transmission coefficient for P-SV section, we implement an algorithm based on equations from 13 to 29 in order to compute the reflection and transmission coefficients for VTI media. Prior to anisotropy consideration, we compute the reflection coefficients of the seismic waves for isotropic media by using anisotropic algorithm with applying constraint ($\delta, \epsilon = 0$) on it. Moreover, reflection coefficients are obtained using isotropic algorithm too based on the Zoeppritz equations in order to substantiate to anisotropic algorithm (Shearer, 1999). However a complete set of the reflection and transmission coefficients are required for accomplishing the 3D modelling but only the reflection coefficients of P-P and SV-SV are considered presently in behalf of the complexity of the reflection and transmission curves for this case. Figure 6a, b show the real and the imaginary part of the reflection coefficients of the reflected P and SV waves when incident P- and SV-waves are considered, respectively, and are obtained by the implementation of degenerated anisotropic and isotropic algorithms. The overlapping of these curves show the feasibility of the anisotropic algorithm for isotropic medium. To obtain these figures, the interface has been considered of the two isotropic medium which follow the condition $\alpha_1 < \alpha_2$, $\beta_1 < \beta_2$ and $(\beta_1, \beta_2) < (\alpha_1, \alpha_2)$ where α_i and β_i are the P- and SV-waves respectively. $i = 1$ corresponds to the upper medium and the lower medium is characterized by $i = 2$. For this condition, it is known that when P-wave encounters at the interface four cases, namely, pre-critical, critical1, critical2, post-critical arise in this situation and can be defined on the basis of the maximum slowness possessed by the body waves in the lower medium. However, reflection and transmission coefficients of P and SV waves remain real in pre-critical situation while become complex beyond the pre-critical,
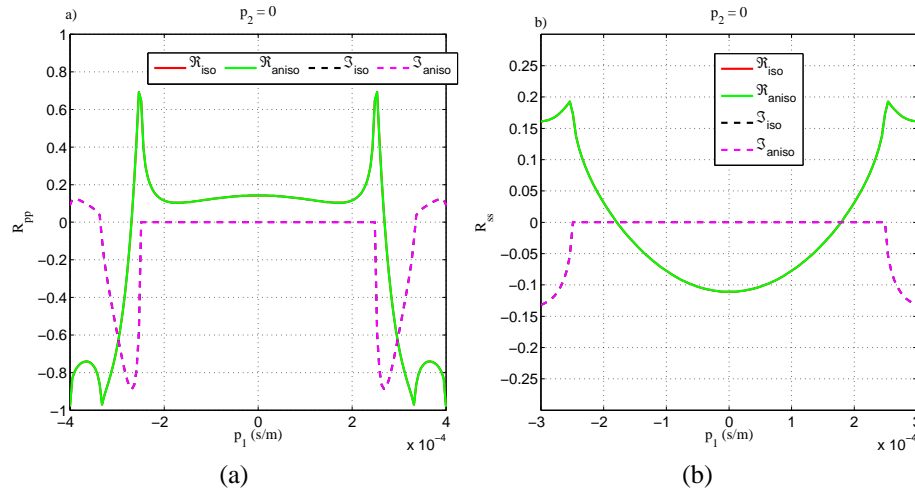
FIG. 6: (a) The real and imaginary part of the R coefficients for (a) P-P (b) S-S cases. The green line denotes the coefficients obtained by degenerated anisotropic algorithm and the red line shows the isotropic coefficients. The dotted black and magenta lines indicates the imaginary part of the R coefficients obtained by the degenerated anisotropic algorithm and isotropic algorithms, respectively. The overlapping of these curve endorse the efficacy of the anisotropic algorithm for isotropic media.

we will consider only pre-critical scenario for further study. As it is known that the better quality and low cost in acquisition and processing of the compressional wave data than the shear wave data make the exploration community to be sophisticated in the acquisition and processing of the P-wave data. In following section, we will consider only P-P reflectivity for seeking the effect of anisotropy on it.

In order to test the accuracy of the plane wave domain reflection coefficient the three models characterized by the class 1, 2 and 3 type of Gas-sand anomaly, respectively are considered. The model parameters used presently are taken from Rüger (Rüger, 2001) and has been published before also by Kim. Further, in order to test the accuracy of the popular approximation given by Rüger is also considered here. Figure 7 shows the P-wave reflectivity with horizontal slowness for a isotropic media. It is indicated from this figure that curves obtained by the exact algorithms of the isotropic media and VTI media are analogous to each other while approximation of Rüger provides a close match to the exact solutions near to the zero horizontal slowness and deviates from the exact solution as slowness increases. The overlapping of the plane wave reflection coefficients obtained by the exact isotropic and degenerated anisotropic algorithms establish the accuracy of the approach followed by the author. Further, the overlay of obtained exact reflection coefficient with the reflection coefficient obtained by applying Rüger's approximation near to the horizontal slowness can be treated as supportive result in favour of the the accuracy of the exact plane wave reflection coefficient given by equations13, 14, 15, 16 and 17. To illustrate the effect of the anisotropy on the P-P reflectivity and the accuracy of the Rüger's approximation's, we show the P-wave reflection coefficients for the same three models as used previously but now the VTI symmetry has been introduced into overburden shale by considering the anisotropic parameters ($\epsilon = 0.133, \delta = 0.12$). Figure 8 illustrate the effect of the anisotropy on the P-P reflection coefficient and accuracy of Rüger's approximation
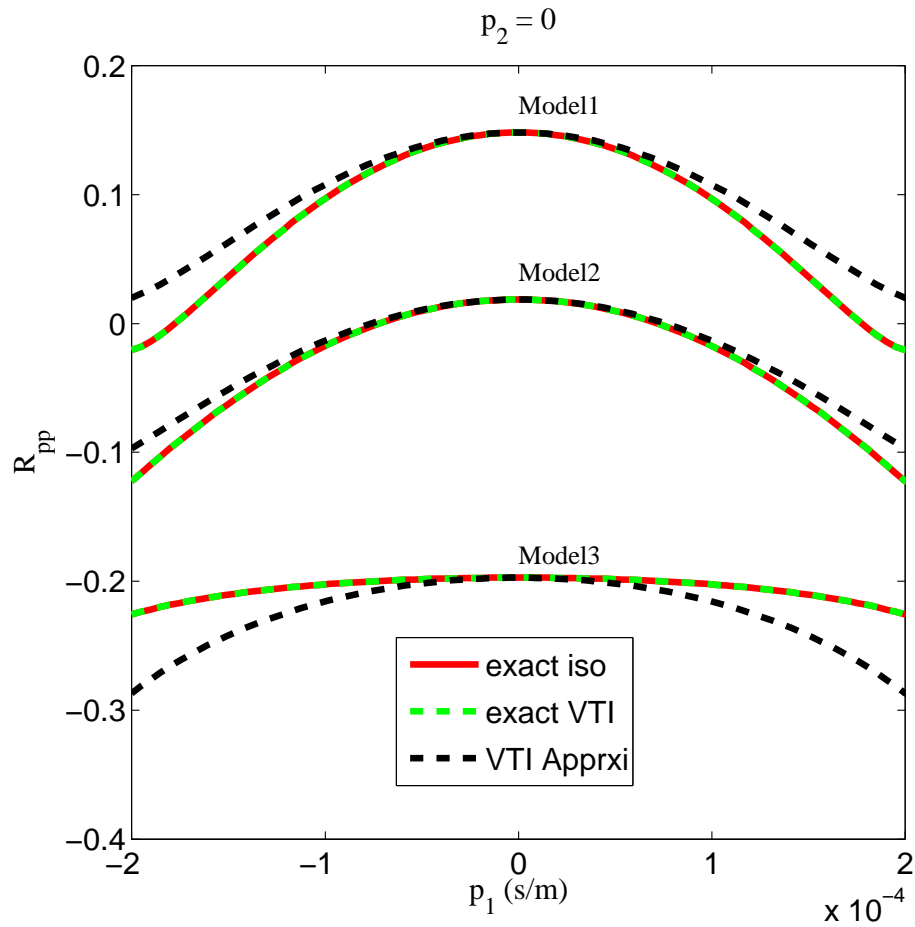
FIG. 7: P-wave reflection coefficients computed for three shale/gas-sand interfaces. The solid red lines indicate the exact solutions and the dashed green and black lines show the solutions computed by exact VTI and Rüger's approximated algorithms for isotropic medium, respectively.
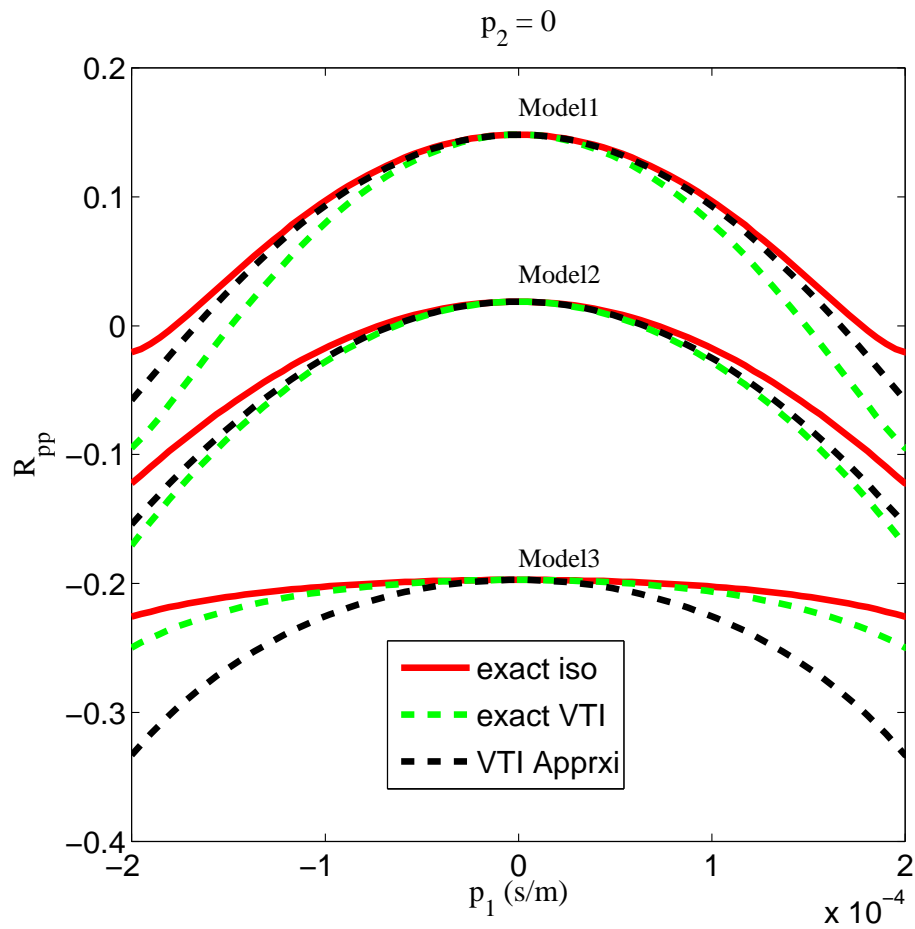
FIG. 8: The reflection coefficients curves of the P-wave for the three models shown in appendix. The thick red line denotes the exact isotropic reflection coefficient, the dashed green and black lines show the exact and approximated reflection coefficients after introducing vertical transverse isotropy into the shale overburden with anisotropic parameters $(\delta = 0.12, \epsilon = 0.133)$

.
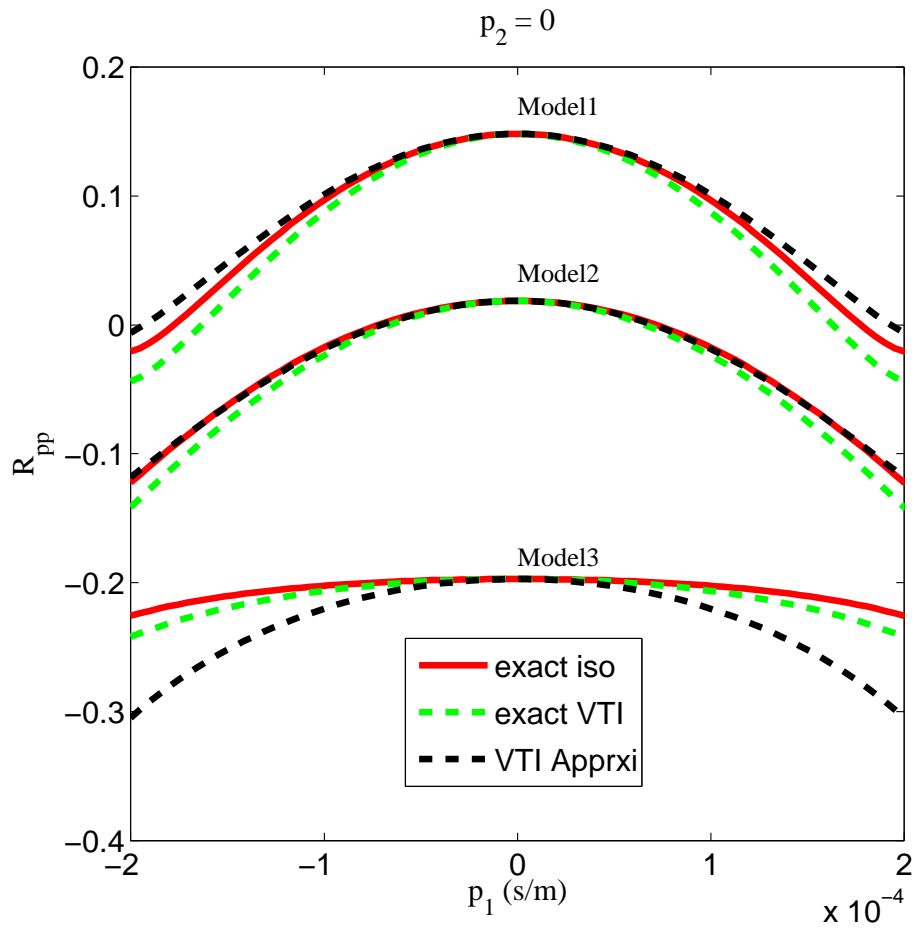
FIG. 9: In order to seek the influence of the ϵ on the reflection coefficients,the same reflection coefficient curves of the P-wave as the ones shown in Figure 8 but for a zero ϵ in the shale layer $(\delta = 0.12, \epsilon = 0)$
.
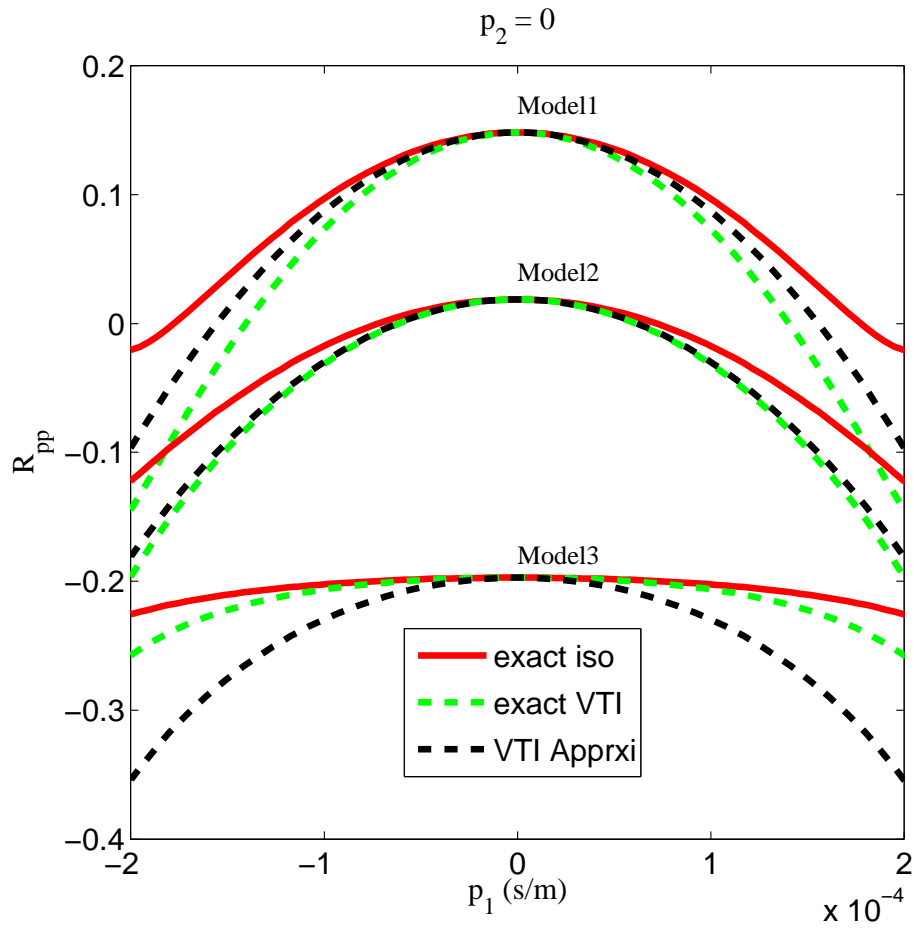
FIG. 10: The same P-wave reflection coefficient curves as shown previously in Figures 8 and 9 but for a VTI medium characterized by anisotropic parameters $(\delta = 0.12, \epsilon = 0.233)$.
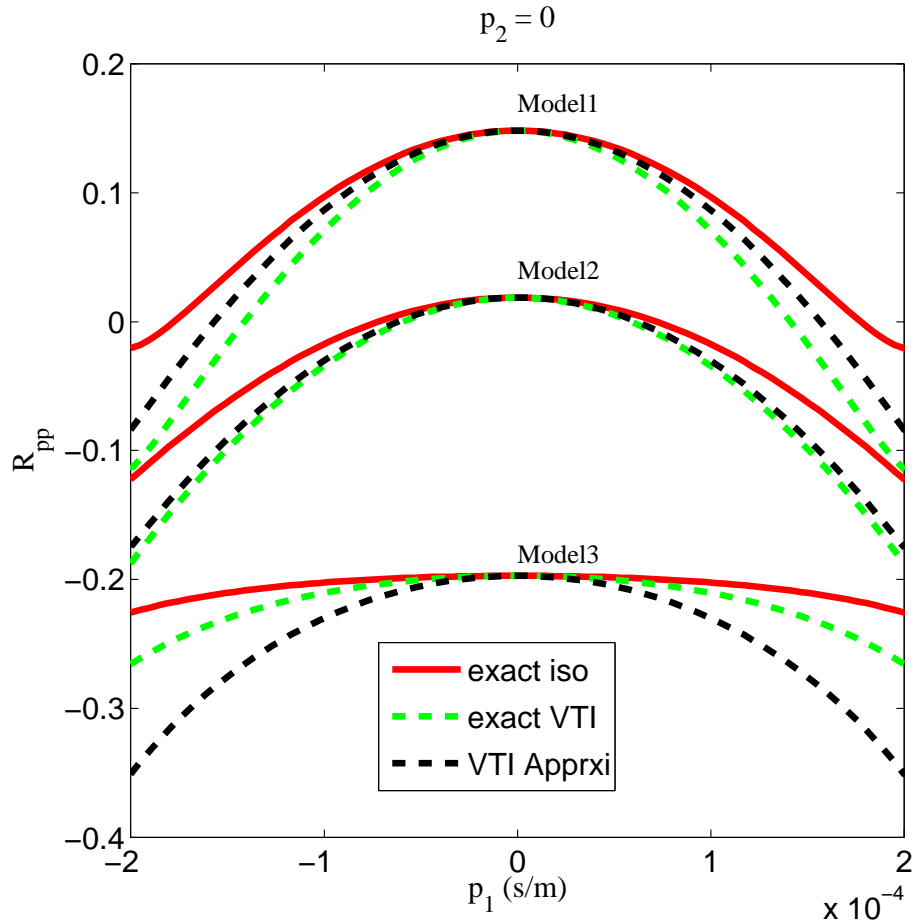
FIG. 11: P-wave reflection coefficient curves for the same three models but for a positive value of δ in the shale layer ($\delta = 0.24, \epsilon = 0.133$)
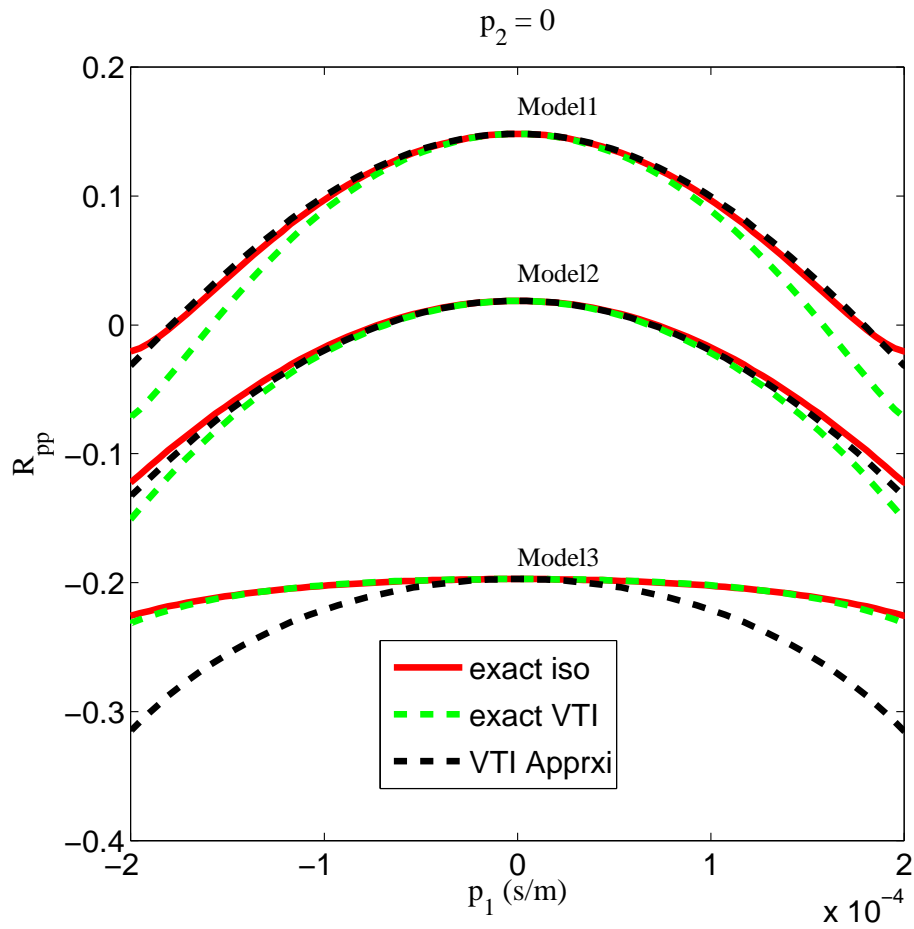
FIG. 12: In order to seek the influence of the δ on the reflection coefficients, the same reflection coefficient curves of the P-wave as the ones shown in Figure 11but for a zero δ in the shale layer $(\delta = 0, \epsilon = 0.133)$
.
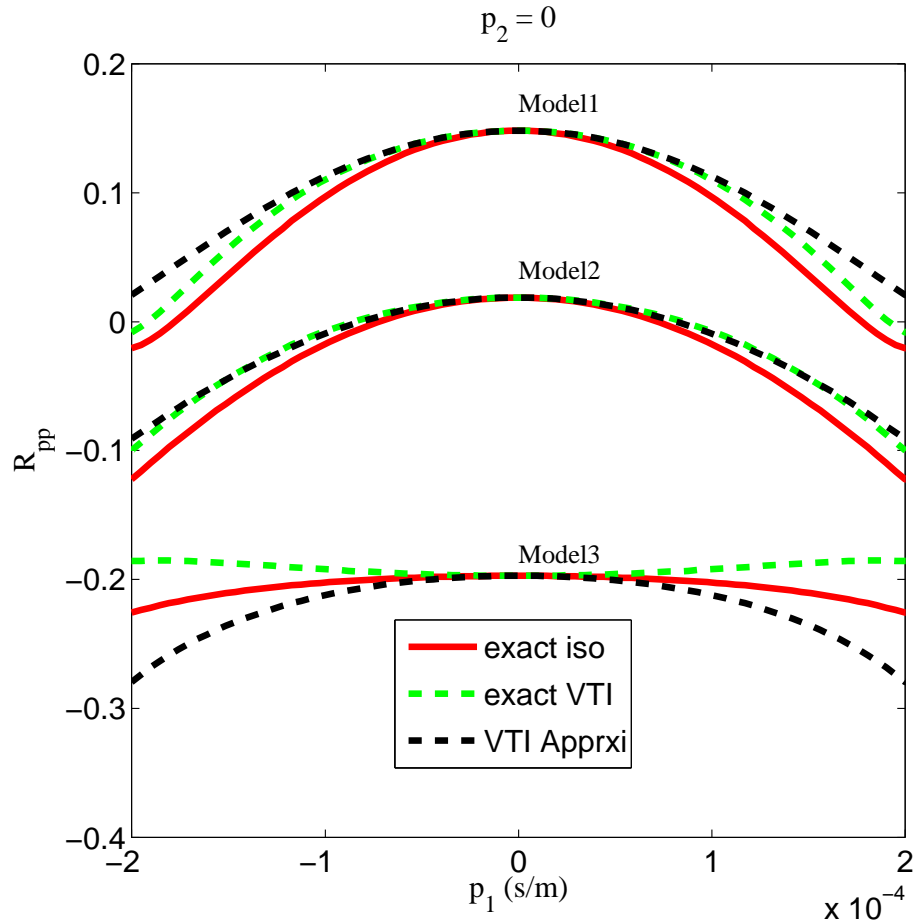
FIG. 13: The same P-wave reflection coefficient curves as the ones shown in Figure11, but for a negative value of anisotropy(negative δ in the overburden ($\delta = -0.24, \epsilon = 0.133$)

as exact VTI reflection coefficient are compared with the corresponding isotropic reflection coefficient ($\epsilon = 0, \delta = 0$) and VTI approximated reflection coefficients. This figure shows that behaviour of the reflection coefficient curve can be changed substantially in the presence of anisotropy. It's also depicted that the VTI approximation's results do match perfectly with the exact one at the zero horizontal slowness and closely near to it. Meanwhile, the deviation of the approximated reflection coefficient curve from the exact one, as horizontal slowness increases, is also observed. It's also noticed that the approximation and the exact reflection curves are close to each other for the first two models. The accuracy of the Rüger's approximation is lower for the third model. In this case it is shown that the anisotropy has its largest influence on the reflection coefficient for higher value of slowness. Further, the examples are repeated for two different value of anisotropy parameter ($\epsilon = 0$ and $\epsilon = 0.233$) in Figures 9 and 10, respectively. By examining these figures it is observed that the difference between the curves are restricted to the large values of slowness but the accuracy of the approximation remains unchanged near to and at the horizontal slowness. Another examples are considered for three different values of anisotropy parameters ($\delta = 0.24$, $\delta = 0$ and $\delta = -0.24$) with constant value of $\epsilon = 0.133$ for observing the influence of delta on the reflection coefficient curves. These examples are shown in the Figures 11, 12 and 13. A close investigation of these Figures makes it possible to illustrate that anisotropy influences the P-wave reflection coefficient in a considerable manner and the difference between the curves near to the zero horizontal slowness is governed by the anisotropy parameter δ.

CONCLUSIONS

We have presented the plane wave reflection coefficient of the SH- and P-SV-waves for anisotropic media by following the Graebner's approach and using effective ray parameter approach in order to accomplish the full elastic wave modelling for anisotropic media in behalf of its efficiency in the plane wave domain. The authentication of the obtained plane wave reflection coefficient of P-wave has been described in reference to isotropic reflection coefficient and Rüger's approximated reflection coefficient. Further, it has been observed that anisotropy influence the solution for the SH-wave reflection coefficient through the contrast in the anisotropy parameter γ across the boundary. It has been demonstrated that anisotropy does not have any effect on the reflection coefficient of the normal incident waves. For P-P case, the parameter δ governs the pattern of the reflection coefficient near to zero slowness and ϵ is responsible for the behaviour of the obtained reflection coefficient at the large values of the horizontal slowness. These observation are a manifestation of the well known facts that ϵ governs the influence of anisotropy on the P-waves travelling near horizontally and δ dominates near vertical wave propagation. If there is no contrast in Thomson's parameters (ϵ, δ) across the interface, the reflection coefficients obtained from the exact anisotropic algorithm by putting an constraint ($\epsilon, \delta = 0$) on it coincides with that obtained from purely isotropic algorithm, meanwhile the reflection coefficient obtained from Rügers approximation do match with the exact one at and near to the zero horizontal slowness. Finally, these analysis of the effect of anisotropy on the reflectivity of the body waves, indicate that conventional AVO analysis needs to be modified in the presence of anisotropy on either side of interface. Since there is considerable difference between the reflection coefficient curve obtained from the exact and approximated algorithms at the large value of the horizontal slowness and this difference may also be noticeable near to

zero slowness in the presence of strong anisotropy, we should deal with the more exact algorithm so that the scanty of the accuracy could be avoided.

REFERENCES

Aki, K., and Richards, P. G., 1980, Quantitative Seismology Theory and Methods: W.H. Freeman and Co.,San Francisco.

Daley, P., and Horn, F., 1977, Reflection and transmission coefficients for transversely isotropic media.: Bulletin of the Seismological Society of America, **67**.

Ferguson, R. J., and Margrave, G. F., 2008, 3D anisotropic phase shift operators: CREWES Research Report, **20**, 2–4.

Graebner, M., 1992, Plane-wave reflection and transmission coefficients for a transversely isotropic solid.: Geophysics, **57**.

Grechka, V., 2009, Application of Seismic Anisotropy in the Oil and Gas Industry.: EAGE.

Kennett, B. L. N., 2001, The Seismic Wavefield.: Cambridge.

Krebes, E. S., 2008, Seismic Theory and Methods: Course Notes.

Rüger, A., 2001, Reflection Coefficient and Azimuthal AVO analysis in Anisotropic Media.: Society of Exploration Geophysicists.

Sharma, R. K., and Ferguson, R. J., 2009, R and t coefficients for sh wave in plane wave domain: CREWES Research Report, **21**.

Shearer, P. M., 1999, Introduction to Seismology: Elesvier.

Slawinski, M. A., 2003, Seismic waves and Rays in Elastic Media.: Pergamon Second Edition.

Thomsen, L., 1986, Weak elastic anisotropy: Geophysics, **51**, No. 10, 1954–1966, discussion in GEO-53-04-0558-0560 with reply by author.

Thomson, L., 2002, Understanding Seismic Anisotropy in Exploration and Exploitation: Distinguished Instructor Series, No 5.

Tsvankin, I., 2001, Seismic Signatures and Analysis of Reflection data in Anisotropic Media.: Handbook of Geophysical Exploration Series.

Upadhyay, S. K., 2004, Seismic Reflection Processing: Springer.

APPENDIX

Parameters	Overburden(Shale)	Lower medium(Sand)
V_p(m/s)	3300	4200
V_s(m/s)	1700	2700
$Density(gm/cm^3)$	2.35	2.49

Table 1: Model parameters for Class 1 AVO

Parameters	Overburden(Shale)	Lower medium(Sand)
V_p(m/s)	2960	3490
V_s(m/s)	1380	2290
$Density(gm/cm^3)$	2.43	2.14

Table 2: Model parameters for Class 2 AVO

Parameters	Overburden(Shale)	Lower medium(Sand)
V_p(m/s)	2730	2020
V_s(m/s)	1240	1230
$Density(gm/cm^3)$	2.35	2.13

Table 3: Model parameters for Class 3 AVO